Nitric Oxide 92 (2019) 41–48

Contents lists available at ScienceDirect

Nitric Oxide

journal homepage: www.elsevier.com/locate/yniox

Sensitive and quantitative method to evaluate DNA methylation of the positive regulatory domains (PRDI, PRDII) and cAMP response element (CRE) in human endothelial nitric oxide synthase promoter

V. Vigorelli[a], E. Rurali[a], S. Carugo[b], G. Pompilio[a,c], M.C. Vinci[a,*]

[a] Unit of Vascular Biology and Regenerative Medicine, Centro Cardiologico Monzino - IRCCS, Milan, Italy
[b] Cardiology Unit, ASST Santi Paolo e Carlo and Department of Health Sciences, University of Milan, Milan, Italy
[c] Dipartimento di Scienze Cliniche e di Comunità, Università degli Studi di Milano, Milan, Italy

ARTICLE INFO

Keywords:
eNOS promoter
DNA methylation
Epigenetics
qPCR

ABSTRACT

Nitric oxide plays a prominent role in the cardiovascular system and much attention has been devoted in the last years on deciphering the regulation of human endothelial nitric oxide synthase (eNOS) expression. Epigenetic-based mechanisms have a key role in the eNOS expression and their pathologic perturbations may have profound effects on the steady state RNA levels in the endothelium. The human eNOS promoter lacks a canonical TATA box and it does not contain a proximal CpG island. A differentially DNA methylated region (DMR) in the native eNOS proximal promoter is involved in gene expression regulation. Here we describe a quantitative, sensitive and cost-effective method that, relying on a novel normalization strategy, allows the quantification of DNA methylation status of the positive regulatory domains (PRDI, PRDII) and cAMP response element (CRE) in human eNOS promoter. This technique will enable to explore the functional relevance of DNA methylation perturbations of eNOS promoter both under pathological and physiological conditions.

1. Introduction

Three isoforms of nitric oxide synthase (NOS) encoded by 3 separate genes on different chromosomes catalyze the production of nitric oxide (NO) in mammals, namely neuronal NOS (NOS1), inducible NOS (iNOS or NOS2), and endothelial NOS (eNOS or NOS3). These NOS isoforms are characterized by different regulation and cell-specific distribution. eNOS is constitutively expressed in the vascular endothelium and responsible for the majority of NO produced [1–3]. NO, as signaling molecule with antithrombotic and antiatherogenic properties, plays a fundamental role in cardiovascular physiology. NO deficiency is known to induce systemic and pulmonary hypertension, abnormal vascular remodeling, defective angiogenesis, pathological healing in response to vascular injury, and impaired mobilization of stem and progenitor cells [4]. Given the prominent role of NO in the cardiovascular system, much attention has been focused on deciphering the regulation of eNOS. To this regard important transcriptional, post-transcriptional, and post-translational mechanisms have been described [5]. Recently, particular emphasis has been placed on epigenetics, as it provides a new observation point for understanding eNOS transcriptional control paradigms in vascular endothelial cells, both in health and disease states [6–8]. The human eNOS promoter lacks a canonical TATA box and it does not contain a proximal CpG island, but a differentially methylated region (DMR) whose DNA methylation status plays an important role in the regulation of the transcription, as well as in the endothelial cell-specific expression of the gene [9]. DNA methylation has been implicated in various cellular processes including transcriptional regulation. Methyl-CpG is recognized as a gene silencing signal and their specific presence at promoter level prevents the interaction of the transcription factors with their binding sites [10–12]. Indeed, whereas non-endothelial cells, such as vascular smooth cells and $CD34^+$ stem cells, are highly methylated at proximal promoter sequences, endothelial cells lack DNA methylation in this same region [6]. The DMR encompasses cis-DNA elements known to be necessary for eNOS transcription, such as the positive regulatory domains I and II (PRDI, PRDII) whose methylation, along with cAMP Response Element (CRE), impedes and regulates eNOS gene transcription [4,13]. Given the important role of DNA methylation in eNOS transcriptional regulation, here we describe a quantitative, sensitive and cost-effective two-step qPCR method to evaluate PRDI, PRDII and CRE methylation status of eNOS promoter. The method, relies on innovative normalization strategy settled by our laboratory for other genes [14,15] that allows

* Corresponding author. Centro Cardiologico Monzino IRCCS, Via Parea 4, I-20138, Milan, Italy.
E-mail address: cristina.vinci@ccfm.it (M.C. Vinci).

https://doi.org/10.1016/j.niox.2019.08.005
Received 20 May 2019; Received in revised form 7 August 2019; Accepted 8 August 2019
Available online 14 August 2019
1089-8603/ © 2019 The Authors. Published by Elsevier Inc. This is an open access article under the CC BY license (http://creativecommons.org/licenses/BY/4.0/).

the detection and quantification of small methylation-density differences between pre-amplified DNA samples. This technique will enable to explore the functional relevance of DNA methylation perturbations of eNOS promoter both under pathological and physiological conditions.

2. Materials and methods

2.1. Cell culture

Primary human cord blood $CD34^+$ cells and human umbilical vein endothelial cells (HUVECs) were obtained from American Type Culture Collection (ATCC). $CD34^+$ stem cells were maintained in StemSpan (StemCell Technologies) containing 50 ng/mL stem cell factor (SCF, Peprotech), 50 ng/mL FMS-Like Tyrosine Kinase 3 (FLT-3, Peprotech), 20 ng/mL for each ligand interleukin (i.e. IL-6, IL-3, Peprotech). HUVECs were maintained in EGM2 medium (Lonza) supplemented with 2 mM L-glutamine, 10% heat-inactivated fetal bovine serum (FBS, Gibco) and 1% penicillin/streptomycin. All cultured cells were incubated at 37 °C with 5% CO_2.

2.2. DNA extraction, whole-genome amplification and fully methylated genomic DNA preparation

Genomic DNA (gDNA) from $CD34^+$ stem cells and HUVECs was isolated by PureLink Genomic DNA kit (Invitrogen) following manufacturer's protocols. Nucleic acid samples were quantified by NanoDrop ND-1000 Spectrophotometer (Thermo Fisher Scientific) and its integrity was analyzed by 1% agarose gel electrophoresis. Whole–genome amplification (WGA) was performed by use of REPLI-g Mini Kit (Qiagen) according to manufacturer's protocol starting from 10 ng of gDNA extracted from primary HUVECs. The WGA product was purified by QIAquick PCR Purification Kit (Qiagen) and quantified with NanoDrop ND-1000 Spectrophotometer. The WGA product was used as fully un-methylated DNA [16]. Fully methylated gDNA (Sss1-DNA) was prepared by treating gDNA from HUVECs with CpG Methyltransferase (M.SssI, New England Biolabs) according to manufacturer's instructions.

2.3. Sodium bisulfite genomic modification

Bisulfite conversion and subsequent purification was performed by MethylCode Bisulfite Conversion Kit (Invitrogen) following manufacturer's protocols, starting from 300 ng of gDNA. After conversion, DNA was eluted in 10 µL (30ng/µL).

2.4. Primers and PCR conditions for two-step PCR

The eNOS gene sequence was obtained from ENSEBL (http://www.ensembl.org) and carefully analyzed to identify the PRDI, PRDII and CRE regions at proximal promoter level, as described by Chan and coworkers [6]. Seven primers for eNOS promoter were designed (Fig. 1): two external methylation independent primers (MIP1Fw, MIP1Rv), one nested forward methylation independent primer (MIP2Fw) for data normalization, and four nested methylation specific primers for the CpGs in CRE (MSP1Fw, MSP1Rv), PRDI and PRDII (MSP2Fw, MSP2Rv) regions. The sequences of both MIP1 primer set and nested MIP2Fw were designed to flank PRDI, PRDII and CRE regions and not to bind CpG dinucleotides. Nested MIP2Fw primer was specifically used only in the second PCR step along with the reverse MIP1Rv primer for data normalization. Nested MSP primers contained at least two CpG sites to render the primers as specific as possible to the methylated template. Primer list is reported in Table 1.

Our two-step method is based on two sequential PCR reactions. The first PCR (MIP1-PCR) is performed with conventional Thermal Cycler (BioRad) in 25 µl reaction mixture composed of 30 ng (if not differently stated) of bisulfite-converted DNA, 0.5 µM for each primer (MIP1Fw, MIP1Rv), 1x PCR Buffer, 200 µM dNTP mix, and 0.5 µL HotStarTaq DNA Polymerase (Qiagen). PCR conditions are 95 °C for 15 min for initial heat activation, followed by 40 cycles of 95 °C for 30s, 57 °C for 45s, 72 °C for 1 min and a final extension cycle of 72 °C for 20 min. The amplification product (879 bp, referred to as input PCR product), purified with the QIAquick PCR Purification Kit (Qiagen), is then quantified by NanoDrop ND-1000 Spectrophotometer and stored at −20 °C for the subsequent step.

The second-step consists of three separate nested qPCR reactions in which the input product of the MIP1-PCR (879 bp) is used as template. Two reactions are performed with nested MSP primer sets (MSP1-qPCR using MSP1Fw/MSP1Rv and MSP2-qPCR using MSP2Fw/MSP2Rv), and one with nested MIP primer set (MIP2-qPCR using MIP2Fw/MIP1Rv). Specifically, 1 µl of purified and diluted input of the MIP1-PCR product was added to 10 µl of qPCR reaction mixture composed of 0.5 µM primer pair and 5 µL SYBR Green Supermix 2X (BioRad). All reactions were performed in separate wells of 96-well reaction plate on CFX96 Real–Time System PCR (Bio-Rad) and the samples analyzed in technical duplicate or triplicate. The qPCR conditions were as follows: 95 °C for 3 min followed by 40 cycles of 95 °C for 15s, 60 °C for 50s with 1 cycle of dissociation step to generate a melting curve. For data analysis samples with Ct above 35 were considered as beyond detection threshold and discarded. The input DNA normalization for the qPCRs was performed with the ΔCt method. The Ct of MIP2-qPCR was subtracted to the Ct of MSP1-qPCR and MSP2-qPCR (ΔCt). The formula $2^{-\Delta Ct}$ was used to calculate the relative amount of methylated DNA in the region investigated by MSP-qPCRs.

2.5. Bisulfite Sanger sequencing

For bisulfite sequencing analysis, the endpoint PCR product from first amplification step of $CD34^+$ stem cells and HUVECs were resolved by 1% agarose gel electrophoresis. The bands of the expected size (879 bp) were excised and purified with QIAquick Gel Extraction Kit (Qiagen), cloned into pCR4-TOPO-TA cloning vector (Invitrogen) and transformed in E. Coli strain DH5α. Ten colonies were randomly picked and directly used for PCR amplification to verify the vector insertion by T3 and T7 primers. Three positive colonies from each sample were Sanger sequenced with T3 primer with the help of an external service (GATC Biotech, Constance, AG). The analysis of sequences was performed with BioEdit software and methylation density assessed and represented by QUMA software (http://quma.cdb.riken.jp/).

2.6. RNA extraction, cDNA preparation and eNOS gene expression analysis by qPCR

Total RNA from primary human cord blood $CD34^+$ stem cells and HUVECs was isolated by use of Direct-zol RNA Kit (Zymo Research) following manufacturer's protocols and quantified by NanoDrop ND-1000 Spectrophotometer. Five hundred ng of total RNA was converted to cDNA with the Superscript III kit (Life Technologies) according to the manufacturer's protocol. The qPCR reactions were performed on CFX96 Real–Time System PCR. The reaction mixtures consisted of 15 µL containing 7.5 µL SYBR Green Supermix, 7.5 ng cDNA and 0.5 µM of each primer. The cycling protocol started with 95 °C for 3 min followed by 40 cycles of 95 °C for 15s, 60 °C for 45s and slow denaturation to generate a melting curve. Relative gene expression was calculated with the ΔCt method. The Ct values of the gene were subtracted (ΔCt) to that of the housekeeping genes (β2-microglobulin). Primer list is reported in Table 1.

2.7. Western Blot

$CD34^+$ stem cells and HUVECs were lysed by RIPA buffer (150 mM NaCl, 50 mM Tris-HCl, 1% NP-40, 0.5% sodium deoxycholate, and

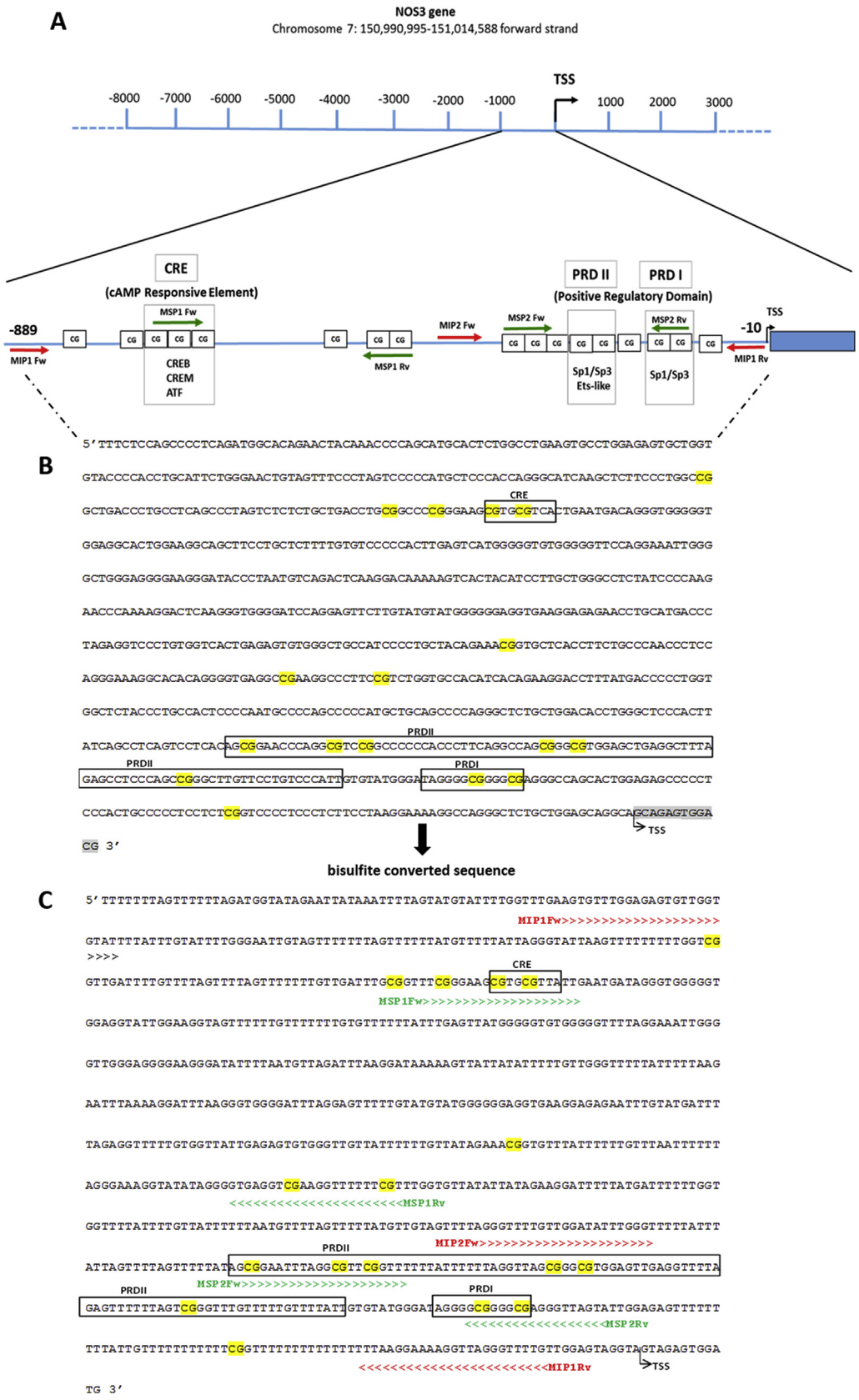

Fig. 1. eNOS gene.
(A) Schematic representation from −889 to −10 bp of human eNOS promoter containing PRDI, PRDII and CRE elements (in the frame). Red and green arrows indicate the annealing position of MIP and MSP primer sets respectively within the analysed region. DNA sequence before **(B)** and after bisulfite treatment **(C)** of the region of interest. In yellow are highlighted CpG dinucleotide resolution involved in eNOS transcription regulation.

Table 1

Bisulfite treated DNA	Name	Sequence 5' —> 3'
	MIP1 Fw	AGTGTTTGGAGAGTGTTGGTGTAT
	MIP1 Rv	ACAAAACCCTAACCTTTTCCTTAAA
	MIP2 Fw	TAGGGTTTTGTTGGATATTTGGGT
	MSP1 Fw	TTCGGGAAGCGTGCGTTA
	MSP1 Rv	ACGAAAAAACCTTCGACCTCAC
	MSP2 Fw	CGGAATTTAGGCGTTCGGTTT
	MSP2 Rv	TACTAACCCTCGCCCCGC
cDNA		
	eNOS Fw	GTGGCTGGTACATGAGCACT
	eNOS Rv	TGGCTAGCTGGTAACTGTGC
	β2-Microglobulin Fw	GGACTGGTCTTTCTATCTCTTGTAC
	β2-Microglobulin Rv	ACCTCCATGATGCTGCTTAC

0.1% SDS) supplemented with a protease inhibitor cocktail (Sigma Aldrich), quantified by Pierce BCA Protein Assay (Thermo Scientific), and then subjected to Western Blot analyses as previously described [17]. The membrane was incubated with a primary antibody specific for eNOS (Sc-654, C-20; Santa Cruz Biotechnology) and then with a peroxidase-conjugated anti-Rabbit IgG secondary antibody (GE Healthcare). Beta-actin expression level was evaluated with a peroxidase-conjugated primary antibody (A3854, AC-15; Sigma Aldrich) and used to normalize eNOS signal. The membrane was developed using enhanced chemiluminescence detection system (Thermo Scientific), acquired with ChemiDoc Imaging System (BioRad), and quantified with Image Lab 6.0.1 (BioRad).

2.8. Statistical analysis

Results were expressed as mean ± SEM. All experiments were performed at least in triplicate, unless stated otherwise. Unpaired two-tailed Students' T-test was performed and a value of $P \leq 0.05$ was considered significant. Statistical analyses were performed and graphs designed utilizing the statistical software GraphPad Prism 5.00 (GraphPad Software).

3. Results

3.1. Principle of the technique

The human eNOS gene has been mapped to the chromosome 7q35-36 [9] and consists of 26 exons spanning 21 kb of gDNA. Two clustered cis-regulatory regions have been identified in the proximal TATA-less eNOS promoter: PRDI (−104/-95 upstream transcription start site (TSS)) and PRDII (−210/-117) that along with CRE region (−740/-731) are known to regulate eNOS transcription [6] (Fig. 1A, B and C). The method schematized in Fig. 2 consists of one conventional PCR followed by three qPCRs. In the conventional PCR (MIP1-PCR) the methylation independent primers (MIP1Fw, MIP1Rv) are first used to specifically amplify a portion of eNOS promoter (from −889 to −10 bp relative to TSS) encompassing the three regions of interest [6]. This MIP1-PCR amplifies an 879 bp long fragment regardless its methylation status (Fig. 2). In the second step the diluted 879 bp endpoint product from the MIP1-PCR (referred to as input PCR product) is subjected to three separate SYBR Green-based qPCRs. In particular, two reactions quantify the methylation status of CRE (398 bp) and PRDI/PRDII (126 bp) regions with the use of nested methylation-specific primers MSP1Fw, MSP1Rv (MSP1-qPCR) and MSP2Fw, MSP2Rv (MSP2-qPCR; Fig. 2, green arrows); while the third reaction (MIP2-qPCR) amplify a 251 bp region by nested methylation independent MIP2Fw and MIP1Rv primers (Fig. 2, red arrows). The cycle thresholds (Ct) deriving from this latter qPCR is used to normalize the Ct from the MSP primer sets and to calculate the relative quantification of methylation status in the samples ($2^{-\Delta Ct}$). After the end of qPCR program a dissociation step is immediately performed for melting curve analysis.

3.2. Sensitivity and accuracy of two-step PCR method

Serial dilutions (0.1 ng/μL to 0.1 fg/μL) of fully methylated DNA, obtained from the pre-amplification of *in vitro* methylated gDNA (Sss1-DNA) converted with bisulfite, were used to evaluate the amplification efficiency (AE, %) and detection limit of MSP1, MSP2 and MIP2 primer sets. Both MSP2 and MIP2 primer sets showed 100% of AE, whereas MSP1 primer set was slightly below (80%, Fig. S1). In line with AE analysis, the detection limit of MSP1 primer sets was 0.1 fg while the same amount was still efficiently amplified by MSP2 and MIP2 primer sets, even if the melting profile of MIP2 end-products revealed an initial primer dimer formation, also confirmed by gel electrophoresis (Fig. S2).

To evaluate the ability of primer sets to discriminate between methylated and un-methylated DNA, as well as the quantification limit and accuracy of the method, *in vitro* Sss1-methylated and WGA un-methylated DNA were bisulfite converted and pre-amplified by MIP1 primer sets. PCR products were then mixed to obtain solutions with the same total DNA concentration, but composed by increasing percentage of methylated DNA. Briefly, input MIP1-PCR products from both Sss1-DNA- and WGA-DNA-PCR were serially diluted to 0.5 ng/μL up to 0.01 pg/μL. Afterwards, the methylated and un-methylated DNA dilutions were properly mixed to obtain solutions containing equal concentration of total DNA (0.5 ng/μL to 0.01 pg/μL) and increasing amount of methylated DNA (0% 20%, 40%, 60%, 80% and 100%). The solutions were then analyzed by two-step PCR method and the data, plotted against their respective methylation percentage, were subjected to linear regression analysis. The analysis revealed a strong linear relationship across the normalized data points and percentage of methylated templates in all used solutions (Fig. 3A and B and Figs. S3A and B). In particular, the lowest total DNA concentration (0.01 pg/μL) still showed a robust amplification signal for both methylated and reference amplicons (Fig. S3A, B and C), demonstrating the ability of this method to detect and reliably quantify as low as 0.002 pg of methylated DNA in 0.01 pg of total DNA template (corresponding to the 20% of methylated DNA in the linear regression analysis). Moreover, the high reproducibility of reference Ct in curves made with DNA solutions ranging from 0.01 pg/μL to 0.5 ng/μL and constituted by increasing amount of methylated DNA, demonstrated that the nested primers used for normalization (MIP2Fw and MIP1Rv) maintained the same amplification efficiency throughout reactions, also in the presence of template with different methylation state (Fig. 3C and Fig. S3C), an essential prerequisite for accurate quantifications.

To further demonstrate the method sensitivity, we directly performed qPCR assays on bisulfite-converted gDNA and compared the results with those obtained with two-step PCR. Ten pg of bisulfite-converted Sss1-methylated gDNA and 10 pg of purified input PCR product, resulting from amplification of bisulfite-converted Sss1-methylated DNA, were used as template in MSP1-qPCR, MSP2-qPCR and MIP2-qPCR. The analysis of the qPCR amplification plots showed that only the Ct value of the reactions performed directly on bisulfite-treated gDNA (one-step PCR) was beyond detection threshold (Ct = 35) in MSP1-qPCR, MSP2-qPCR and 20 cycles higher in MIP2-qPCR when compared with two-step PCR (Fig. 4A). In addition, the analysis of melting curve profiles of endpoint PCR products showed unspecific amplification products or primer dimer formation when bisulfite-treated gDNA samples were directly used in the assay but not with the two-step method (Fig. 4B, C and D). The melting curve data were further confirmed by gel electrophoretic analysis of PCR endpoint products (inserts in Fig. 4B, C and D). Taken together these data show that the inclusion of a first amplification step in the assay enables the analysis of bisulfite-treated gDNA quantities that, when directly analyzed by the one-step PCR approach, result in no product formation or in very late

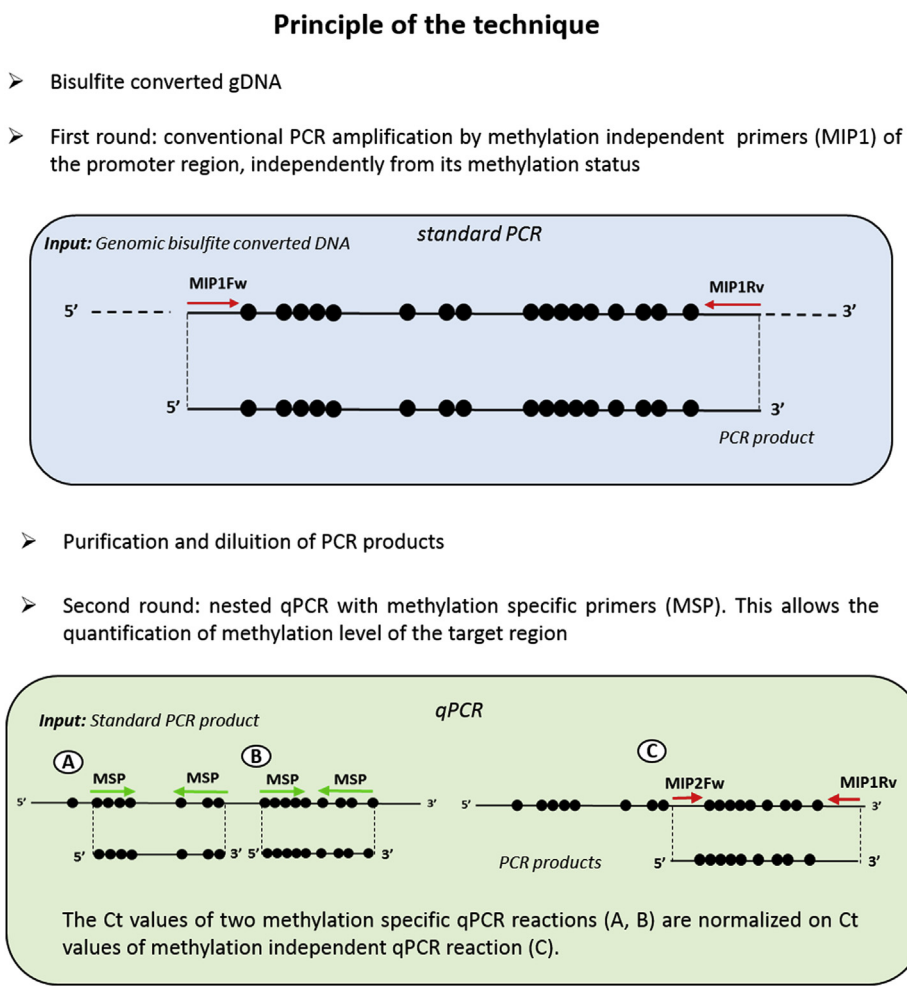

Fig. 2. Method overview.
Schematic diagram of technique based on two step PCR. Bisulfite-converted gDNA is used as template in the first amplification of 879 bp region encompassing PRDI, PRDII and CRE elements (MIP1Fw and MIP1Rv). Nested qPCR consists of three independent reactions performed with diluted input PCR product from the first PCR round. Two nested methylation specific primer reactions (MSP1-qPCR and MSP2-qPCR, in green arrows) evaluate the methylation status of target template. The third methylation independent reaction (MIP2-qPCR, in red arrows) is used as reference control to normalize the amount of methylated target detected by the MSP-qPCRs with the ΔCt method. Black circles (•) are a schematic representation of methylated CpG.

threshold cycles, thus allowing DNA methylation profiling from small amounts of gDNA starting material. Moreover, the two-step PCR approach eliminates both primer dimer formation and the possibility of false priming on non-specific templates, overcoming a frequent problem observed in direct gDNA amplification [18,19]. Therefore, as already demonstrated with a nested PCR approach [20], this method showed higher sensitivity and specificity in target template detection than one-step PCR. All in all, this technique allows a relative quantification of DNA methylation and, once positive and negative controls are assessed, the samples under investigation can be analyzed and compared.

3.3. Method validation and melting profile analysis of qPCR products

To validate the quantification efficiency of the method in biological samples we analyzed two cell types characterized by low/null and high eNOS expression: $CD34^+$ stem cells and HUVECs [6,21]. Bisulfite treated gDNA isolated from the cells was used to investigate the methylation status of CRE and PRDI/PRDII regions of eNOS promoter (Fig. 5A). As expected all analyzed regions displayed high methylation levels in $CD34^+$ stem cells and null/low in HUVECs (Fig. 5B and C).

The results were further confirmed at nucleotide resolution level by bisulfite Sanger sequencing, the “gold standard” method in methylation studies. After sequencing the number of methylated sites and percentage of methylation were assessed. As shown in Fig. 6A data deriving from bisulfite Sanger sequencing were consistent with those obtained by the two-step PCR method, thus confirming its validity. Consistently, eNOS mRNA and protein expression in HUVECs and $CD34^+$ stem cells (Fig. 6B and C) correlated with the methylation level of CRE and PRDI/PRDII regions.

The melt profile of qPCR endpoint products was also analyzed (Fig. 6D, E and F). While MSP1-qPCR and MSP2-qPCR end products deriving from both HUVECs and $CD34^+$ stem cells displayed similar melting temperature, MIP2-qPCR products differed considerably. Specifically, the melt temperature of $CD34^+$ stem cell amplicons was two grades higher than that of HUVECs (78 °C vs 76 °C, respectively; Fig. 6F). Bisulfite-converted DNA templates harboring various degrees of methylation at their CpG sites generate amplicons with distinct melting temperatures. Generally, the higher is the GC-content the higher is the melting temperature. In line, amplicons of fully methylated $CD34^+$ stem cell templates were characterized by a right-shifted melting profile, whereas HUVECs showed a left-shifted melting indicating that all CpG sites were not methylated. Therefore, the analysis and interpretation of melting curves can also serve as useful and effective strategy to assess the methylation density of CpG sites on target template. All qPCR end products were also resolved on 1% agarose gel to confirm the presence of only one band of the expected size (inserts in Fig. 6D, E and F).

4. Discussion

Chan and coworkers demonstrated that DNA methylation is important in controlling transcription of eNOS gene [6]. This epigenetic modification is extensively studied and numerous techniques have been developed for its investigation [22,23]. The most common PCR-based DNA methylation techniques comprise methylation specific PCR (MSP), MethyLight and methylation-sensitive high resolution melting (MS-HRM) and bisulfite sequencing PCR (BSP and cloning-based BSP). All these techniques include, as first step, the conversion of the DNA with

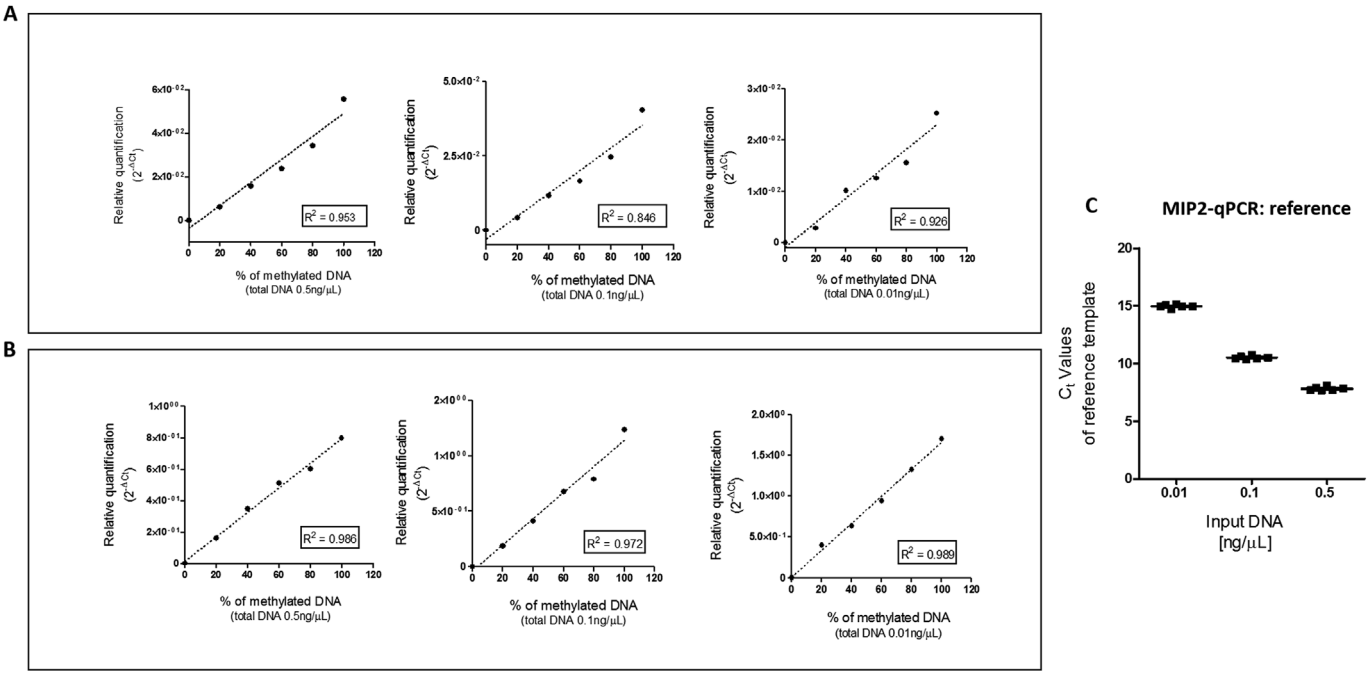

Fig. 3. Quantitative accuracy of the two-step PCR method.
Linear regression analysis between normalized quantification and percentage of methylated template for MSP1-qPCR **(A)** and MSP2-qPCR primer sets **(B)** for 0.5, 0.1, 0.01 ng/µL of total input DNA. For each data point three independent reactions were performed. The correlation coefficient (R^2) are indicated on the plotted graph. **(C)** Reproducibility of reference Ct in curves made with increasing amount of input PCR product (0.01 ng/µL to 0.5 ng/µL) constituted by increasing amount of methylated DNA. For every input of total DNA each dot represents a different percentage of methylated DNA (0%, 20%, 40%, 60%, 80% and 100%).

bisulfite [24] and have as intrinsic characteristic the inability to discriminate 5 mC and 5hmC [25]. MSP, although simple and highly sensitive technique [26], is not a quantitative method and can lead to an overestimation of methylation state especially when looking for very low methylation differences. MSP has been upgraded to quantitative assay by the use of fluorescent TaqMan probe designed for the methylated region of interest and a reference gene for normalization (MethyLight technique) [27]. In this case any signal from non-specific amplification is eliminated. However, the design of the assay can be complicated by the introduction of the probe. Moreover, the use of primers and probes specific for completely methylated templates may lead to failure of the assay or to biased quantitative results when heterogeneous methylation patterns with large variations between consecutive CpGs complementary to the probe are present [27]. The normalization data of MethyLight technique relies on reference genes amplified from bisulfite converted-DNA that is more prone to PCR bias and biased results because of its low sequence diversity.

While BSP techniques holds several technical challenges such as poor signal quality and low sensitivity [28], cloning-based BSP is more accurate, but requires at least six sequencing reactions to obtain meaningful results, and the data obtained are referred to as DNA–-methylation haplotypes [29,30]. Although considered the “gold standard method” in methylation studies, cloning-based BSP is an expensive and time-consuming technique that requires a large number of samples

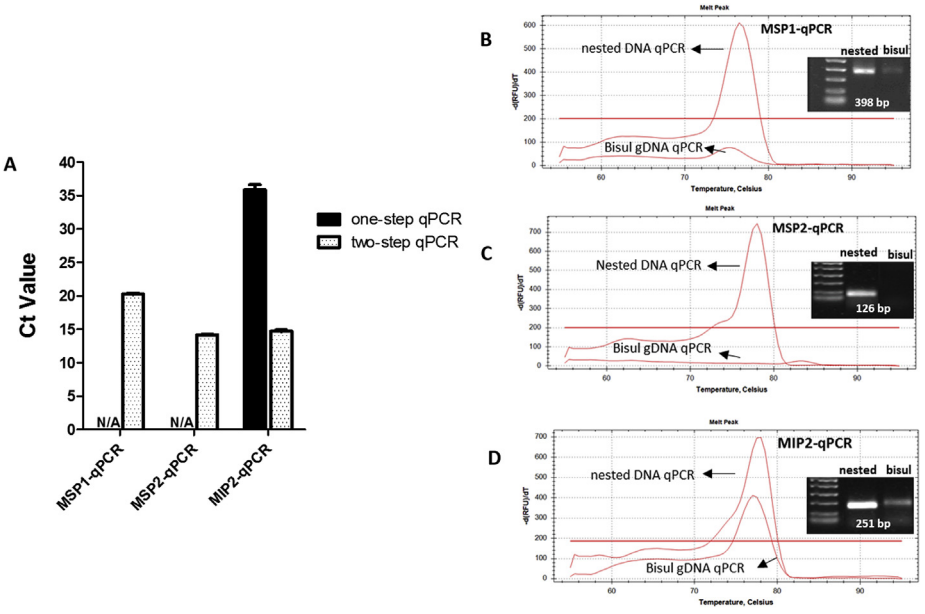

Fig. 4. Sensitivity of the two-step PCR method.
(A) MSP1-qPCR, MSP2-qPCR and MIP2-qPCR performed on input PCR product (two-step PCR) had significantly higher sensitivity than qPCR performed directly on bisulfite-converted gDNA (one-step PCR). Ct values from 10 pg of input PCR products obtained from bisulfite-converted gDNA appeared earlier than in the direct amplification of 10 pg of bisulfite-converted gDNA. **(B, C and D)** Melting curve profiles of endpoint PCR products generated from bisulfite-converted gDNA and two-step qPCR. The inserts represent gel electrophoretic analysis of PCR endpoint products to confirm the absence of nonspecific amplicons formation.

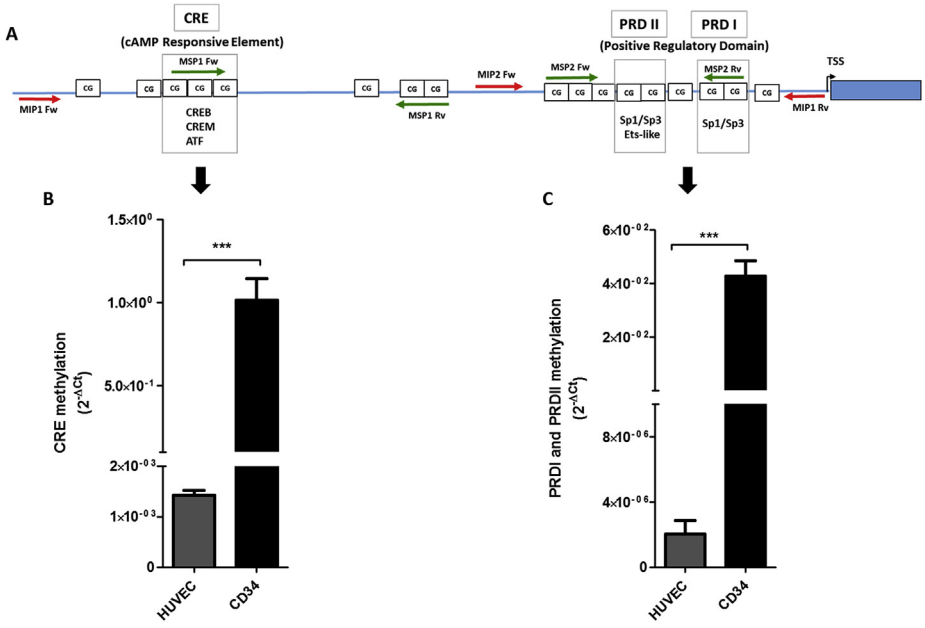

Fig. 5. Method validation on biological samples.
(A) Schematic representation from −889 to −10 bp of human eNOS promoter containing PRDI, PRDII and CRE elements. Methylation status of PRDI, PRDII and CRE elements in CD34$^+$ stem cells and HUVECs obtained by the two-step PCR method using **(B)** MSP1-qPCR and **(C)** MSP2-qPCR primer set (***$p < 0.001$ *vs.* CD34$^+$ stem cells by unpaired *t*-test).

and sequences in order to obtain significant results especially when very small methylation differences need to be detected. Our two-step PCR method set up to investigate the methylation status of CRE and PRDI/PRDII regions of eNOS promoter combines quantitative and melting curve profiling analysis. Both designed MSP primer sets recognize the 70% of 5 mC involved in the regulation of eNOS gene transcription indicating the screening efficiency of the technique. The introduction of a first amplification step makes this method highly sensitive, specific and accurate allowing the detection of as low as 500 pg of bisulfite-converted gDNA (roughly corresponding to the DNA content of 100 cells). As previously demonstrated [14], the pre-amplification of a genomic fragment, which includes both the target sequence

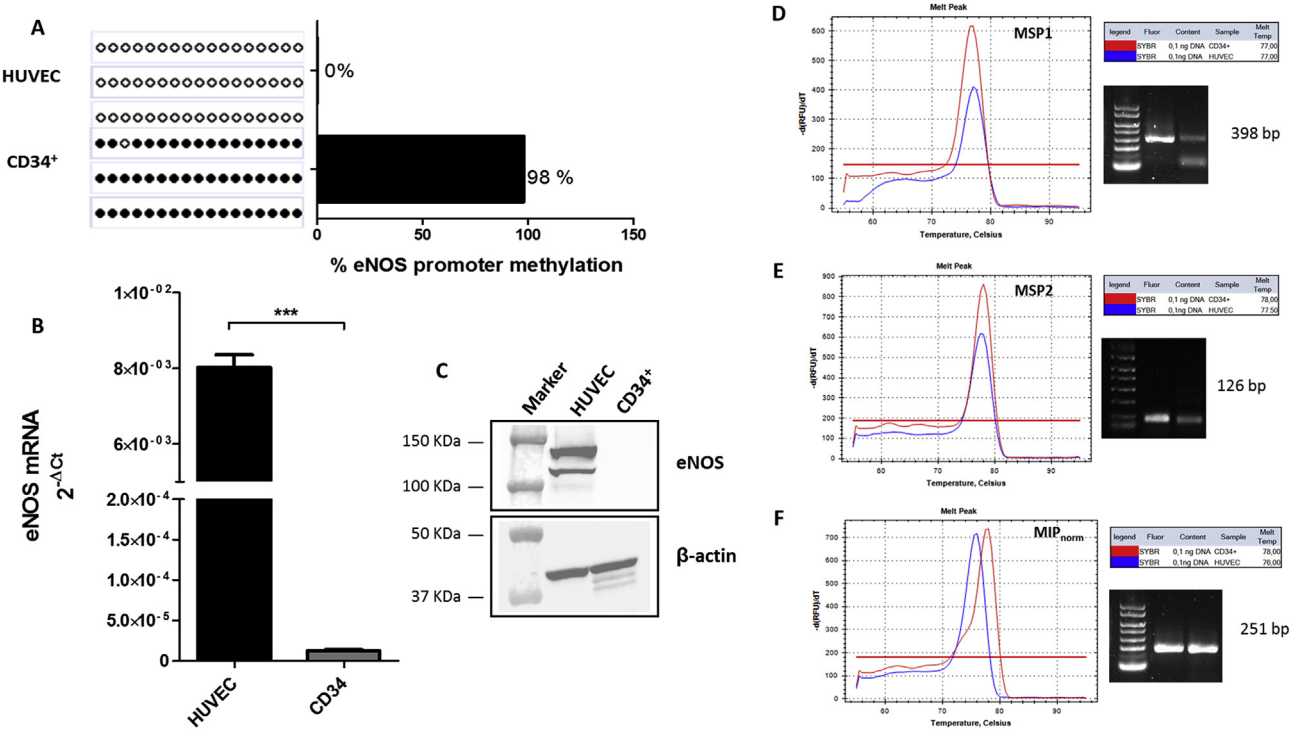

Fig. 6. Method validation by bisulfite Sanger sequencing.
(A) Sanger sequencing of the region of interest (879 bp) amplified by MIP1 primer set. Three randomly selected sequences representative of CpG methylation in PRDI, PRDII and CRE elements in HUVECs and CD34$^+$ stem cells are reported. Open dots are un-methylated cytosine, whereas methylated cytosine are indicated with black dots. On the right, methylation percentage of eNOS promoter in HUVECs and CD34$^+$ stem cells, respectively obtained after QUMA software analysis, are indicated. **(B)** Analysis of eNOS mRNA expression in CD34$^+$ stem cells and HUVECs by qPCR. Data are reported as $2^{-\Delta Ct}$ (***$p < 0.001$ *vs.* CD34$^+$ stem cells by unpaired *t*-test). **(C)** eNOS protein expression level in CD34$^+$ stem cells and HUVECs by Western Blot. Representative melting curve profiles of **(D)** MSP1-qPCR, **(E)** MSP2-qPCR and **(F)** MIP2-qPCR products from un-methylated (HUVECs) and fully methylated (CD34$^+$ stem cells) template. In the inserts, agarose gel electrophoresis analysis of each PCR endpoint products to confirm the presence of only one band of the expected size.

and the reference control, allows a robust quantification of the methylation and reduces qPCR normalization bias [30]. The expression of eNOS is very tightly regulated by epigenetic mechanisms whose perturbations in disease may have profound effects on eNOS steady state RNA levels in the endothelium. Indeed, decreases in eNOS mRNA expression in cardiovascular have been well documented [31–35]. Nevertheless, the epigenetic mechanisms sustaining eNOS expression deficit are not well understood. Here we provide a simple, sensitive and reliable experimental tool useful to study eNOS DNA methylation in a variety of physiological and pathophysiological contexts that require a real-time PCR instrument only.

Conflicts of interest

The authors declare no conflict of interest.

Author contributions

All authors contributed to the work in this paper. M.C.V. conceived, designed the experiments, analyzed the data and wrote the manuscript. V.V. performed the experiments. E.R. contributed in the experiment execution and critically reviewed the final version of the manuscript. G.P. and S.G. provided intellectual suggestions and critically reviewed the manuscript.

Funding

This work was supported by the Ministero della Salute (Ricerca Finalizzata PE-2011-02348537).

Vigorelli's fellowship was supported by Ministero della Salute (PE-2011-02348537).

Appendix A. Supplementary data

Supplementary data to this article can be found online at https://doi.org/10.1016/j.niox.2019.08.005.

References

[1] L.J. Ignarro, G.M. Buga, K.S. Wood, R.E. Byrns, G. Chaudhuri, Endothelium-derived relaxing factor produced and released from artery and vein is nitric oxide, Proc. Natl. Acad. Sci. U. S. A. 84 (1987) 9265–9269.

[2] R.M. Palmer, A.G. Ferrige, S. Moncada, Nitric oxide release accounts for the biological activity of endothelium-derived relaxing factor, Nature 327 (1987) 524–526.

[3] J.E. Fish, P.A. Marsden, Endothelial nitric oxide synthase: insight into cell-specific gene regulation in the vascular endothelium, Cell. Mol. Life Sci. 63 (2006) 144–162.

[4] C.C. Matouk, P.A. Marsden, Epigenetic regulation of vascular endothelial gene expression, Circ. Res. 102 (2008) 873–887.

[5] V. Garcia, W.C. Sessa, Endothelial NOS: perspective and recent developments, Br. J. Pharmacol. 176 (2019) 189–196.

[6] Y. Chan, J.E. Fish, C. D'Abreo, S. Lin, G.B. Robb, A.M. Teichert, F. Karantzoulis-Fegaras, A. Keightley, B.M. Steer, P.A. Marsden, The cell-specific expression of endothelial nitric-oxide synthase: a role for DNA methylation, J. Biol. Chem. 279 (2004) 35087–35100.

[7] J.E. Fish, C.C. Matouk, A. Rachlis, S. Lin, S.C. Tai, C. D'Abreo, P.A. Marsden, The expression of endothelial nitric-oxide synthase is controlled by a cell-specific histone code, J. Biol. Chem. 280 (2005) 24824–24838.

[8] G.B. Robb, A.R. Carson, S.C. Tai, J.E. Fish, S. Singh, T. Yamada, S.W. Scherer, K. Nakabayashi, P.A. Marsden, Post-transcriptional regulation of endothelial nitric-oxide synthase by an overlapping antisense mRNA transcript, J. Biol. Chem. 279 (2004) 37982–37996.

[9] F. Karantzoulis-Fegaras, H. Antoniou, S.L. Lai, G. Kulkarni, C. D'Abreo, G.K. Wong, T.L. Miller, Y. Chan, J. Atkins, Y. Wang, P.A. Marsden, Characterization of the human endothelial nitric-oxide synthase promoter, J. Biol. Chem. 274 (1999) 3076–3093.

[10] R. Klose, A. Bird, Molecular biology. MeCP2 repression goes nonglobal, Science 302 (2003) 793–795.

[11] R. Jaenisch, A. Bird, Epigenetic regulation of gene expression: how the genome integrates intrinsic and environmental signals, Nat. Genet. 33 (Suppl) (2003) 245–254.

[12] J.G. Herman, S.B. Baylin, Gene silencing in cancer in association with promoter hypermethylation, N. Engl. J. Med. 349 (2003) 2042–2054.

[13] K. Niwano, M. Arai, N. Koitabashi, S. Hara, A. Watanabe, K. Sekiguchi, T. Tanaka, T. Iso, M. Kurabayashi, Competitive binding of CREB and ATF2 to cAMP/ATF responsive element regulates eNOS gene expression in endothelial cells, Arterioscler. Thromb. Vasc. Biol. 26 (2006) 1036–1042.

[14] V. Bianchessi, A. Lauri, V. Vigorelli, M. Toia, M.C. Vinci, Evaluating the methylation status of CXCR4 promoter: a cost-effective and sensitive two-step PCR method, Anal. Biochem. 519 (2017) 84–91.

[15] V. Vigorelli, J. Resta, V. Bianchessi, A. Lauri, B. Bassetti, M. Agrifoglio, M. Pesce, G. Polvani, G. Bonalumi, L. Cavallotti, F. Alamanni, S. Genovese, G. Pompilio, M.C. Vinci, Abnormal DNA methylation induced by hyperglycemia reduces CXCR 4 gene expression in CD 34(+) stem cells, J. Am. Heart. Assoc. 8 (2019) e010012.

[16] V. Bianchessi, M.C. Vinci, P. Nigro, V. Rizzi, F. Farina, M.C. Capogrossi, G. Pompilio, V. Gualdi, A. Lauri, Methylation profiling by bisulfite sequencing analysis of the mtDNA Non-Coding Region in replicative and senescent Endothelial Cells, Mitochondrion 27 (2016) 40–47.

[17] E. Rurali, C.A. Pilato, G.L. Perrucci, A. Scopece, I. Stadiotti, D. Moschetta, M. Casella, E. Cogliati, E. Sommariva, G. Pompilio, P. Nigro, Cyclophilin a in arrhythmogenic cardiomyopathy cardiac remodeling, Int. J. Mol. Sci. 20 (2019).

[18] M.W. Chan, E.S. Chu, K.F. To, W.K. Leung, Quantitative detection of methylated SOCS-1, a tumor suppressor gene, by a modified protocol of quantitative real time methylation-specific PCR using SYBR green and its use in early gastric cancer detection, Biotechnol. Lett. 26 (2004) 1289–1293.

[19] H. Thomassin, C. Kress, T. Grange, MethylQuant: a sensitive method for quantifying methylation of specific cytosines within the genome, Nucleic Acids Res. 32 (2004) e168.

[20] F.G. Abath, F.L. Melo, R.P. Werkhauser, L. Montenegro, R. Montenegro, H.C. Schindler, Single-tube nested PCR using immobilized internal primers, Biotechniques 33 (2002) 1210–1212 1214.

[21] K. Ohtani, G.J. Vlachojannis, M. Koyanagi, J.N. Boeckel, C. Urbich, R. Farcas, H. Bonig, V.E. Marquez, A.M. Zeiher, S. Dimmeler, Epigenetic regulation of endothelial lineage committed genes in pro-angiogenic hematopoietic and endothelial progenitor cells, Circ. Res. 109 (2011) 1219–1229.

[22] H. Heyn, M. Esteller, DNA methylation profiling in the clinic: applications and challenges, Nat. Rev. Genet. 13 (2012) 679–692.

[23] L.S. Kristensen, M.B. Treppendahl, K. Gronbaek, Analysis of epigenetic modifications of DNA in human cells, Chapter 20, Curr. Protoc. Hum. Genet. (2013) Unit20 2.

[24] I.L. Candiloro, T. Mikeska, A. Dobrovic, Closed-tube PCR methods for locus-specific DNA methylation analysis, Methods Mol. Biol. 791 (2011) 55–71.

[25] Y. Huang, W.A. Pastor, Y. Shen, M. Tahiliani, D.R. Liu, A. Rao, The behaviour of 5-hydroxymethylcytosine in bisulfite sequencing, PLoS One 5 (2010) e8888.

[26] S. Derks, M.H. Lentjes, D.M. Hellebrekers, A.P. de Bruine, J.G. Herman, M. van Engeland, Methylation-specific PCR unraveled, Cell. Oncol. 26 (2004) 291–299.

[27] C.A. Eads, K.D. Danenberg, K. Kawakami, L.B. Saltz, C. Blake, D. Shibata, P.V. Danenberg, P.W. Laird, MethyLight: a high-throughput assay to measure DNA methylation, Nucleic Acids Res. 28 (2000) E32.

[28] M. Jiang, Y. Zhang, J. Fei, X. Chang, W. Fan, X. Qian, T. Zhang, D. Lu, Rapid quantification of DNA methylation by measuring relative peak heights in direct bisulfite-PCR sequencing traces, Lab. Investig. 90 (2010) 282–290.

[29] J. Lewin, A.O. Schmitt, P. Adorjan, T. Hildmann, C. Piepenbrock, Quantitative DNA methylation analysis based on four-dye trace data from direct sequencing of PCR amplificates, Bioinformatics 20 (2004) 3005–3012.

[30] H.G. Hernandez, M.Y. Tse, S.C. Pang, H. Arboleda, D.A. Forero, Optimizing methodologies for PCR-based DNA methylation analysis, Biotechniques 55 (2013) 181–197.

[31] D. Won, S.N. Zhu, M. Chen, A.M. Teichert, J.E. Fish, C.C. Matouk, M. Bonert, M. Ojha, P.A. Marsden, M.I. Cybulsky, Relative reduction of endothelial nitric-oxide synthase expression and transcription in atherosclerosis-prone regions of the mouse aorta and in an in vitro model of disturbed flow, Am. J. Pathol. 171 (2007) 1691–1704.

[32] A. Giaid, D. Saleh, Reduced expression of endothelial nitric oxide synthase in the lungs of patients with pulmonary hypertension, N. Engl. J. Med. 333 (1995) 214–221.

[33] B.J. Krause, P.M. Costello, E. Munoz-Urrutia, K.A. Lillycrop, M.A. Hanson, P. Casanello, Role of DNA methyltransferase 1 on the altered eNOS expression in human umbilical endothelium from intrauterine growth restricted fetuses, Epigenetics 8 (2013) 944–952.

[34] N.C. Harvey, K.A. Lillycrop, E. Garratt, A. Sheppard, C. McLean, G. Burdge, J. Slater-Jefferies, J. Rodford, S. Crozier, H. Inskip, B.S. Emerald, C.R. Gale, M. Hanson, P. Gluckman, K. Godfrey, C. Cooper, Evaluation of methylation status of the eNOS promoter at birth in relation to childhood bone mineral content, Calcif. Tissue Int. 90 (2012) 120–127.

[35] A. Daiber, N. Xia, S. Steven, M. Oelze, A. Hanf, S. Kroller-Schon, T. Munzel, H. Li, New therapeutic implications of endothelial nitric oxide synthase (eNOS) function/dysfunction in cardiovascular disease, Int. J. Mol. Sci. 20 (2019).